

Preparation, Characterization, and In Vitro and In Vivo Evaluation of Lovastatin Solid Lipid Nanoparticles

Submitted: May 5, 2006; Accepted: August 2, 2006; Published: March 23, 2007

Gande Suresh,¹ Kopparam Manjunath,¹ Vobalaboina Venkateswarlu,¹ and Vemula Satyanarayana²

¹NDDS Laboratory, University College of Pharmaceutical Sciences, Kakatiya University, Warangal—506 009, Andhra Pradesh, India

²Dr Reddy's Laboratories, Hyderabad, Andhra Pradesh, India

ABSTRACT

The purpose of this research was to study whether the bioavailability of lovastatin could be improved by administering lovastatin solid lipid nanoparticles (SLN) duodenally to rats. Lovastatin SLN were developed using triglycerides by hot homogenization followed by ultrasonication. Particle size and zeta potential were measured by photon correlation spectroscopy. The solid state of the drug in the SLN and lipid modification were characterized. Bioavailability studies were conducted in male Wistar rats after intraduodenal administration of lovastatin suspension and SLN. Stable lovastatin SLN having a mean size range of 60 to 119 nm and a zeta potential range of -16 to -21 mV were developed. More than 99% of the lovastatin was entrapped in the SLN. Lovastatin was dispersed in an amorphous state, and triglycerides were in β^1 form in the SLN. In vitro stability studies showed the slow release and stability of lovastatin SLN. The relative bioavailabilities of lovastatin and lovastatin hydroxy acid of SLN were increased by $\sim 173\%$ and 324% , respectively, compared with the reference lovastatin suspension.

KEYWORDS: Solid lipid nanoparticles, lovastatin, differential scanning calorimetry, powder x-ray.

INTRODUCTION

Presently, many research groups are trying to explore the possibility of using solid lipid nanoparticles (SLN) as drug carriers. The concept of SLN was first investigated a decade ago to unravel problems associated with other colloidal drug delivery systems, such as instability and nonbiodegradability. SLN are widely used to improve bioavailability and to achieve sustained release.¹ Lovastatin lowers cholesterol levels through reversible and competitive inhibition of 3-hydroxy-3-methylglutaryl coenzyme A reductase, an enzyme involved

in the biosynthesis of cholesterol. It exhibits poor oral bioavailability ($<5\%$) because of rapid metabolism in the gut and liver. Cytochrome P450 3A4 metabolizes the lactone form of lovastatin into hydroxy acid and its metabolites.² To overcome hepatic first-pass metabolism and to enhance bioavailability, intestinal lymphatic transport of drugs can be exploited. Transport of drugs through the intestinal lymphatics via the thoracic lymph duct to the systemic circulation at the junction of the jugular and left subclavian vein, avoids pre-systemic hepatic metabolism and therefore enhances bioavailability. Highly lipophilic compounds such as long-chain triglycerides reach systemic circulation via the lymphatics. Lovastatin (whose water solubility is 0.4×10^{-3} mg/mL) is considered to be a reasonable substrate for intestinal lymphatic transport because of its high log P value (4.3) and good solubility in oils (38 and 42 mg/mL in carbitol and propylene glycol monocaprylate, respectively).

Lipid-based drug delivery systems enhance the bioavailability of lipophilic drugs such as halofantrine and ontazolast by lymphatic transport of biosynthesized chylomicrons associated with the drugs.^{3,4} Another approach for lymphatic transport of nano- and microparticles is by particular uptake by M cells of Peyer's patches.⁵⁻⁹ Nanoparticles coated with hydrophobic polymers tend to be easily captured by lymphatic cells in the body.¹⁰ Intraduodenally administered tobramycin-loaded SLN showed sustained release and lymphatic targeting.¹¹ The main aim of this study was to improve the bioavailability of lovastatin by preparing lovastatin SLN using trimyristin (TM) and tripalmitin (TP), by hot homogenization followed by ultrasonication. Differential scanning calorimetry (DSC) and powder x-ray diffractometry (PXRD) analyses were performed to investigate the status of the lipid and the drug. In vitro stability and bioavailability of formulations were assessed.

MATERIALS AND METHODS

Materials

Lovastatin USP, simvastatin, and lovastatin hydroxy acid were obtained from Dr Reddy's Laboratories (Hyderabad, India). TM (Dynasan 114) and TP (Dynasan 116) were generously supplied by Sasol (Witten, Germany). Soy phosphatidylcholine 95% (Epikuron 200) was donated by Degussa

Corresponding Author: Vobalaboina Venkateswarlu, NDDS Laboratory, University College of Pharmaceutical Sciences, Kakatiya University, Warangal—506 009, Andhra Pradesh, India. Tel: +91 870 2439299; Fax: +91 870 2438844; E-mail: vobala@yahoo.com

Texturant Systems (Hamburg, Germany). Poloxamer 188 (Pluronic F 68) and dialysis membrane-70 were purchased from HiMedia (Mumbai, India). Centriscart filters (molecular weight cutoff 20 000 Da) were purchased from Sartorius (Goettingen, Germany).

Preparation of Lovastatin SLN and Suspension

SLN were prepared by a hot homogenization followed by ultrasonication method as described previously.¹² Lovastatin (0.1% wt/vol), triglyceride (2% wt/vol), and phosphatidylcholine 95% (1.5% wt/vol) were dissolved in a 10-mL mixture of chloroform and methanol (1:1). Organic solvents were completely removed using a Buchi rotoevaporator (Buchi Labortechnik AG, Flawil, Switzerland). The drug-embedded lipid layer was melted by heating 5°C above the melting point of the lipid. An aqueous phase was prepared by dissolving poloxamer 188 (1% wt/vol) in double-distilled water (sufficient to produce 20 mL of preparation) and heating to the same temperature as the oil phase. The hot aqueous phase was added to the oil phase, and homogenization was performed (at 6000 rpm and 70°C) using a Diax 900 homogenizer (Heidolph Electro, Kelheim, Germany) for 3 minutes. The coarse hot-oil-in-water emulsion so obtained was ultrasonicated (12T-probe) using a Sonopuls ultrahomogenizer (Bandelin, Berlin, Germany) for 25 minutes. Lovastatin SLN were obtained by allowing the hot nanoemulsion to cool to room temperature. Blank and lovastatin SLN prepared with TM and TP are abbreviated as BL-TM and BL-TP, and LOV-TM and LOV-TP, respectively.

Lovastatin and methylcellulose mucilage (0.5% wt/vol) was ground in a mortar to obtain a 1 mg/mL lovastatin suspension; this suspension was ultrasonicated for 2 minutes. The average particle size ($n = 300$) was measured using an optical microscope and found to be $2.43 \pm 1.26 \mu\text{m}$.

Measurement of Size and Zeta Potential of SLN

The size and zeta potential of SLN were measured by photon correlation spectroscopy using a Zetasizer 3000 HSA (Malvern, UK). Samples were diluted appropriately with the aqueous phase of the formulation for the measurements, and the pH of diluted samples ranged from 6.9 to 7.2. Zeta potential measurements were done at 25°C, and the electric field strength was around 23.2 V/cm.

Assay and Entrapment Efficiency

For estimation of assay, 0.2 mL of formulation was diluted to 10 mL with chloroform/methanol (1:1). The final dilution was made with the mobile phase, and lovastatin content was determined by high performance liquid chromatography (HPLC). Ultracentrifugation was performed using a Centriscart

(8000 rpm for 30 minutes), which consists of a filter membrane (molecular weight cutoff 20 000 Da) at the base of a sample recovery chamber to separate the dispersion medium. The entrapment efficiency of the system was determined by measuring the concentration of free drug in the dispersion medium by HPLC, as mentioned below.

The chromatographic system consisted of a Shimadzu LC-10AT solvent delivery pump (Kyoto, Japan) equipped with a 20- μL loop and a UV visible detector. A Kromasil (Alltech Associates Inc, Columbia, Maryland) (250 \times 4.6 mm) analytical column was used. The mobile phase consisted of an aqueous buffer (ammonium phosphate [0.05 M] and phosphoric acid [0.01M]) and acetonitrile (40:60). The column temperature was maintained at 50°C, and the flow rate was kept at 2 mL/min. The eluate was monitored at 238 nm, and the sensitivity selected was 0.001 absorbance units at full scale. Data were recorded using Winchrom software (GBC Scientific Equipment, Victoria, Australia).

Stability Studies

Lovastatin SLN of TM and TP (1% poloxamer 188) were stored at 25°C for 6 months, and average size and entrapment efficiency were determined. The number of samples estimated was 3.

Characterization by DSC and PXRD

The samples used for these analyses were (1) lovastatin; (2) triglycerides; (3) physical mixtures: PM_{1:20} (drug:triglyceride, 1:20) and PM_{1:1} (drug:triglyceride, 1:1); and (4) mixtures obtained by solvent evaporation (SM_{1:20}). Lyophilized SLN:trehalose solution 30% wt/vol was used as a cryoprotectant. DSC analysis was performed using a Mettler DSC (Mettler-Toledo, Viroflay, France) by taking a 10-mg sample. A heating rate of 10°C/min was employed in the range of 30°C to 230°C. Analysis was performed under a nitrogen purge (50 mL/min). The powder x-ray diffractometer Siemens D-5000 (Karlsruhe, Germany) was used for diffraction studies. PXRD studies were performed on the samples by exposing them to $\text{CuK}\alpha_1$ radiation (50 kV, 34 mA) and scanning from 3° to 35° and 2θ at a step size of 0.02°. The amount of pure drug taken for PXRD analysis is equivalent to that present in PM and SM.

In Vitro Stability Studies

In vitro stability studies were performed using a modified Franz diffusion cell at 37°C. A dialysis membrane having a pore size of 2.4 nm and a molecular weight cutoff between 12 000 and 14 000 was used. The membrane was soaked in double-distilled water for 12 hours before mounting in a Franz diffusion cell. Lovastatin SLN (1 mL) were placed in

the donor compartment, and the receptor compartment was filled with dialysis medium (12 mL of phosphate buffer pH 6.8). At fixed time intervals, 100 μ L of the sample was withdrawn from the receiver compartment through a side tube and analyzed by HPLC as described above.

Animals and Intraduodenal Administration of Lovastatin Formulations

Male Wistar rats (200 \pm 20 g) (NIN, Hyderabad, India) were used for the study. Animals were kept under fasting overnight prior to the experiment. All experimental procedures were reviewed and approved by the animal and ethics review committee of the Faculty of Pharmaceutical Sciences, Kakatiya University (Warangal, India). Euthanasia and disposal of the carcass were in accordance with the guidelines. Rats were anesthetized by an intraperitoneal injection of 60 mg/kg of thiopentone sodium. A small incision was made in the abdomen, the duodenum was located, and lovastatin formulations were administered gently into the duodenum with a syringe at 10 mg/kg. The muscle and skin of the main incision were sutured carefully. Blood samples were drawn by retroorbital venous plexus puncture at 15, 30, 45, 60, 90, 120, 240, and 360 minutes after the intraduodenal dose. The samples were collected in heparinized Eppendorf tubes and centrifuged (5000 rpm, 15 minutes), and plasma was collected and stored at -20°C until analysis.

Plasma Sample Processing and Liquid Chromatography-Mass Spectroscopy/Mass Spectroscopy (LC-MS/MS) Analysis of Lovastatin

Owing to the instability of lovastatin in rat plasma at ambient temperature, all sample preparations were performed on an ice-water bath. For the extraction of the drug and the internal standard (simvastatin) we have employed the solid-phase extraction method reported by Wu et al.¹³ Briefly, the sample was loaded onto the Solid Phase Extraction (C8) (Waters, Milford, MA) and low vacuum was applied; then the cartridge was washed with 1 mL each of water, 5% formic acid, and water separately, followed by 1 minute of drying. Each cartridge was then eluted with 1 mL of methanol-water (70:30) and 1 mL of acetonitrile separately. The combined eluates (1 mL of methanol-water and 1 mL of acetonitrile) were evaporated to dryness under reduced pressure in a vacuum oven. Residues were reconstituted in 50 μ L of ammonium acetate (1 mM, pH 4.0)–acetonitrile (30:70) and then vortexed for 1 minute. The reconstituted sample was transferred into auto sampler (Gilson 215, Middleton, Wisconsin) vials, and 20 μ L of the sample was injected onto the LC column.

The processed plasma samples were analyzed using a triple-quadrupole LC-MS/MS mass spectrometer (API 3000) equipped with an ion-spray LC-MS interface and an Agilent

1100 quaternary pump (Agilent Technologies, Waldbronn, Germany). Separation was performed on an Advanced Chromatography Technologies 3C18 column (50 \times 4.5 mm) (MAC-MOD Analytical Inc, Chadds Ford, PA) with mobile-phase aqueous ammonium acetate (1 mM, pH 4.0) and acetonitrile (40:60), at a flow rate of 1 mL/min. The mass spectrometer was operated in the negative ion mode for the first 3 minutes and then switched to the positive mode for the rest of the run.

Pharmacokinetics and Statistical Analysis

Plasma concentration vs time data for lovastatin and lovastatin hydroxy acid in individual rats were analyzed by noncompartmental estimations using WinNonlin software (version 1.1). Relative bioavailability ($Fr\%$) of lovastatin and lovastatin hydroxy acid were obtained using the following equation:

$$Fr \% = \frac{AUC_{0-\infty}(SLN)}{AUC_{0-\infty}(Suspension)} \times 100 \quad (1)$$

where AUC is area under the curve.

Pharmacokinetic parameters of lovastatin after intraduodenal administration of LOV-suspension and LOV-TP, and of lovastatin hydroxy acid after intraduodenal administration of LOV-suspension and LOV-TP, were compared by Student *t* test, using SPSS (version 11.0, SPSS Inc, Chicago, Illinois).

RESULTS AND DISCUSSION

Preparation of SLN

In the preparation of SLN, triglyceride 2% wt/vol was required to entrap lovastatin at a concentration of 0.1% wt/vol. Solvent system chloroform:methanol (1:1) was used to disperse the lovastatin homogeneously in the lipid. Heating the drug to 70°C in the preparation of SLN could not have affected its stability, because temperature was found to have no significant effect on the rate of hydrolysis of lovastatin, and lovastatin exposed to an oxygen atmosphere (135°C , 15 minutes) was shown to be stable.¹⁴ After homogenization for 3 minutes, optimum average sizes of 3.99 μm and 3.92 μm were obtained for TM and TP SLN, respectively. Average particle size was reduced to below 1 μm by ultrasonication. Sonication time was optimized to 20 minutes to obtain SLN in the range of 60 to 119 nm with a narrow size distribution.

Measurement of Size, Zeta Potential, Entrapment Efficiency, and Assay

Sizes of blank and lovastatin SLN of TM and TP with different percentages of poloxamer 188 are shown in Figure 1. As the poloxamer 188 concentration increased from 0.5% to 1.0%, the mean particle size decreased. In all the formulations,

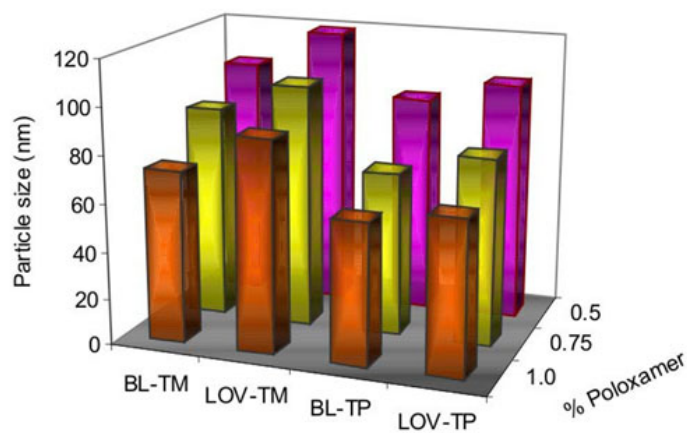


Figure 1. Effect of poloxamer 188 concentration (0.5%, 0.75%, and 1.0%) on particle size of blank and lovastatin SLN of TM and TP. SLN indicates solid lipid nanoparticles; TM, trimyristin; TP, tripalmitin; BL, blank; LOV, lovastatin.

the optimum size (60.1–89.8 nm) was obtained at the 1% poloxamer concentration. The zeta potential of lovastatin SLN was slightly lower than that of blank SLN (Table 1). The entrapment efficiency of lovastatin SLN was more than 99%, and assay values ranged from 0.964 to 0.972 mg/mL.

Stability Data

After 6 months of storage at 25°C, the average size of LOV-TM dispersions increased from 85.3 ± 1.2 nm to 131.5 ± 1.6 nm; similarly, the average size of LOV-TP dispersions increased from 62.2 ± 1.5 nm to 94.4 ± 1.9 nm. The entrapment efficiency lowered from 99.4 ± 0.31 to 97.0 ± 0.26 and from 99.5 ± 0.25 to 98.6 ± 0.28 in the case of LOV-TM and LOV-TP, respectively. Although an increase in the particle size and a decrease in the entrapment efficiency were observed, the values were still good enough for the stability of SLN to be maintained. Transitions of dispersed lipid from the metastable form to the stable form might occur slowly on storage because of small particle size and the presence of emulsifier, and these transitions might lead to drug expulsion from SLN.¹⁵ Therefore, the lowered entrapment efficiency observed during storage may be due to drug expulsion during lipid modification (ie, transformation of higher-energy α and β' modifications to the lower-energy β modification).

During long-term storage, triglycerides undergo degradation to fatty acids and mono- and diglycerides, which could

compete with formulation surfactants for positioning on the surface. Fatty acids and monoglycerides can form mixed micelles that might enhance the partitioning of hydrophobic drug out of the SLN.¹⁶ Therefore, the concentration of excipients and possible degradation products need to be determined to understand the stability of SLN.

DSC

A sharp melting peak of lovastatin at 164.89°C (Figure 2) indicated its crystalline nature. The thermograms of the lyophilized LOV-TM, SM_{1:20}, and PM_{1:20} did not show the melting peak for the lovastatin. This absence might be due to solubilization of low amounts of the drug in molten lipid while the sample was heating up. The presence of the melting peak of lovastatin in PM_{1:1} of LOV-TM supports the notion that having a very low amount of the drug made it difficult to record the melting peak. A similar trend was observed in the case of lovastatin mixtures with TP. There was no melting peak for lovastatin in lyophilized LOV-TP (Figure 2). However, to investigate the state of the drug in lyophilized SLN, PXRD studies were performed, and these showed the amorphous state of the drug. DSC analysis of camptothecin SLN prepared by high-pressure homogenization showed that camptothecin was in an amorphous state.¹⁷

The degree of crystallinity of lyophilized SLN was calculated by comparing the enthalpy of SLN with the enthalpy of bulk lipid.^{18,19} The crystallinity of LOV-TP (72.53%) was greater than that of LOV-TM (30.9%). The degree of crystallinity of TM in the mixtures was as follows: PM_{1:20} (97.58%) > SM_{1:20} (96.78%) > PM_{1:1} (95.48%) > lyophilized LOV-TM (30.9%). A similar order was observed for TP mixtures' crystallinities (Table 2). The melting points of TM and TP in the case of corresponding lyophilized SLN were 52.8°C and 58.4°C, respectively. These melting points were depressed when compared with those of the corresponding bulk triglycerides (Table 2). This suggests that triglycerides in SLN might be in the β' form. However, there was no depression of the melting point of triglyceride in corresponding PM and SM. PXRD results showed that peak intensities for lovastatin in SM were reduced, which suggests that there were fewer chances for the drug to crystallize separately from the lipid. In spite of this, there was no depression of the melting point of triglyceride in SM. We expect that melting point depression was due to the small particle size

Table 1. Size, Zeta Potential, Entrapment Efficiency, and Assay of SLN of Different Triglycerides (mean \pm SD, n = 3)*

SLN	Size (nm)		Polydispersity Index		Zeta Potential (mV)		Entrapment Efficiency (%)	Assay (mg/mL)
	BL	LOV	BL	LOV	BL	LOV		
Trimyristin	85.3 ± 1.2	89.8 ± 0.9	0.168 ± 0.04	0.182 ± 0.025	-21.4 ± 0.9	-17.3 ± 0.7	99.4 ± 0.31	0.964 ± 0.04
Tripalmitin	62.2 ± 1.5	65.6 ± 0.3	0.113 ± 0.03	0.134 ± 0.012	-20.8 ± 2.1	-15.8 ± 0.8	99.5 ± 0.25	0.972 ± 0.03

*SLN indicates solid lipid nanoparticles; BL, blank; LOV, lovastatin.

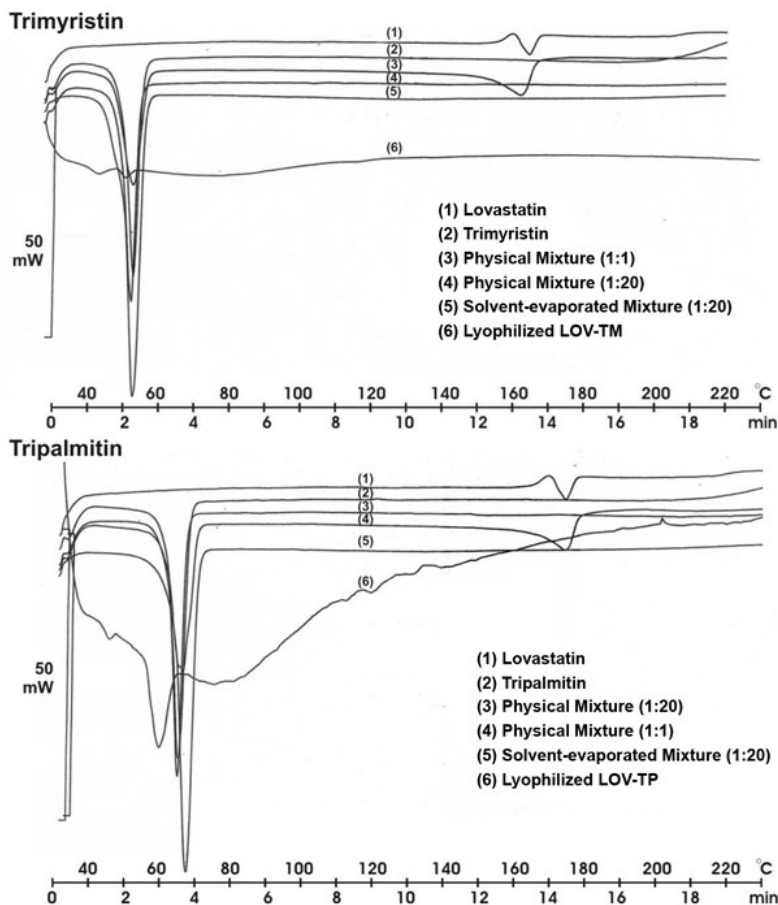


Figure 2. Overlaid differential scanning calorimetry thermograms. LOV indicates lovastatin; TM, trimyrustin; TP, tripalmitin.

(nanometer range), the high specific surface area, and the presence of surfactant—in other words, the depression can be attributed to the Kelvin effect.²⁰ Kelvin realized that small, isolated particles would melt at a temperature lower than the melting temperature of bulk materials. The depression of melting point is in proportion to the curvature $1/r$ of a spherical nanoparticle, according to the Gibbs-Thomson equation.²¹

PXRD

The PXRD pattern of lovastatin exhibited sharp peaks at 2θ scattered angles 9.38, 10.86, 15.66, 16.68, and 18.9, indicating the crystalline nature of lovastatin (Figure 3). The

peak intensities of lovastatin in $PM_{1:20}$ and $SM_{1:20}$ were reduced at 2θ scattered angles 9.38 and 10.86, respectively. This showed that the degree of crystallinity of lovastatin was reduced in PM and SM. The degree of crystallinity was compared on the basis of peak intensities. However, there were no characteristic peaks for lovastatin in vacuum-dried and lyophilized LOV-TM at corresponding 2θ scattered angles (Figure 3). This suggests that lovastatin was in not a crystalline state but an amorphous state in SLN. Similarly, the degree of crystallinity of lovastatin was reduced in the PM and SM of TP. The absence of characteristic peaks for lovastatin indicated that lovastatin was in an amorphous form in vacuum-dried and lyophilized LOV-TP. In our previous

Table 2. Crystallinity of Triglycerides in Mixtures and Lyophilized SLN*

	Parameter	Bulk	$PM_{1:20}$	$PM_{1:1}$	$SM_{1:20}$	Lyophilized SLN
Trimyrustin	Melting peak (°C)	57.92	56.89	56.20	57.72	52.82
	Enthalpy (j/g)	204.98	190.47	97.86	188.91	3.67
	Crystallinity (%)	100	97.58	95.48	96.78	30.9
Tripalmitin	Melting peak (°C)	64.21	63.96	63.84	66.52	58.40
	Enthalpy (j/g)	196.31	183.20	94.27	181.71	8.23
	Crystallinity (%)	100	98.0	96.05	97.2	72.53

* $PM_{1:20}$ and $SM_{1:20}$ contained 95.23% triglyceride, $PM_{1:1}$ contained 50% triglyceride, and lyophilized SLN contained 5.78% triglyceride. The degree of crystallinity of PM, SM, and lyophilized SLN were calculated by comparing their enthalpy with the enthalpy of the corresponding bulk triglyceride. SLN indicates solid lipid nanoparticles; PM, physical mixtures; SM, mixtures obtained by solvent evaporation.

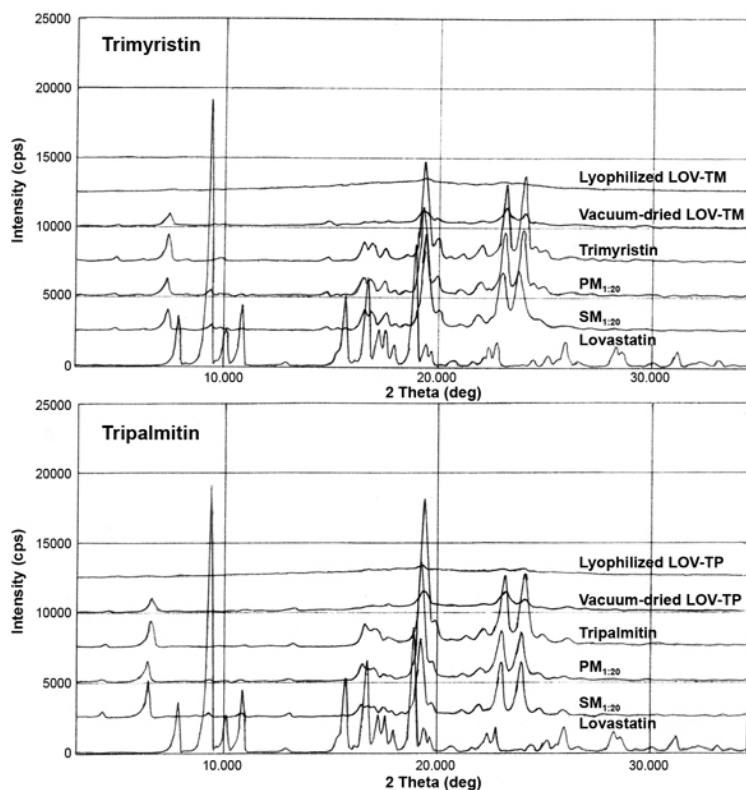


Figure 3. Overlaid powder x-ray diffractometry patterns. LOV indicates lovastatin; TM, trimyrustin; PM, physical mixtures; SM, mixtures obtained by solvent evaporation; TP, tripalmitin.

studies it was shown that clozapine in the SLN formulation was in an amorphous state.¹² In the preparation of SLN, lipid and lovastatin were dissolved in a mixture of solvents, and subsequently solvents were evaporated. This allowed homogeneous dispersion of the drug in the lipid. This confirms that our method of preparation (homogenization followed by ultrasonication) and the presence of surfactants did not allow the drug to crystallize. Similar results were reported by Cavalli et al,^{22,23} who found that rapid quenching of the microemulsion prevents the drug from crystallizing.

The PXRD pattern of TM showed sharp peaks at 2θ scattered angles 19.28, 19.42, 23.18, and 24.04 (Figure 3), indicating the crystalline state of TM. These characteristic peaks were reduced in PM, SM, and vacuum-dried LOV-TM. In the case of lyophilized LOV-TM, the peaks were further reduced. The degree of crystallinity was as follows: $PM_{1:20} > SM_{1:20} > \text{vacuum-dried LOV-TM} > \text{lyophilized LOV-TM}$. This indicates that TM was in a crystalline state in PM, SM, and vacuum-dried and lyophilized LOV-TM. Similarly, TP was in crystalline form in PM, SM, and vacuum-dried and lyophilized SLN.

In Vitro Stability of Lovastatin SLN

Figure 4 shows the percentage of lovastatin and lovastatin hydroxy acid released from LOV-TM and LOV-TP. There was no release of lovastatin hydroxy acid and lovastatin from

SLN until 6 and 12 hours, respectively. Less than 2.0% of lovastatin was released from the lovastatin SLN of TM and TP after 36 hours. Lovastatin that was released from SLN in the dialysis media of phosphate buffer pH 6.8 was converted into lovastatin hydroxy acid. Less than 3.0% of lovastatin hydroxy acid was released from both formulations after 36 hours. The hydrolysis of the lactone ring of lovastatin occurs readily in aqueous solutions, especially under acidic or alkaline conditions. However, the acid-catalyzed hydrolysis is reversible and the rate of equilibrium is pH

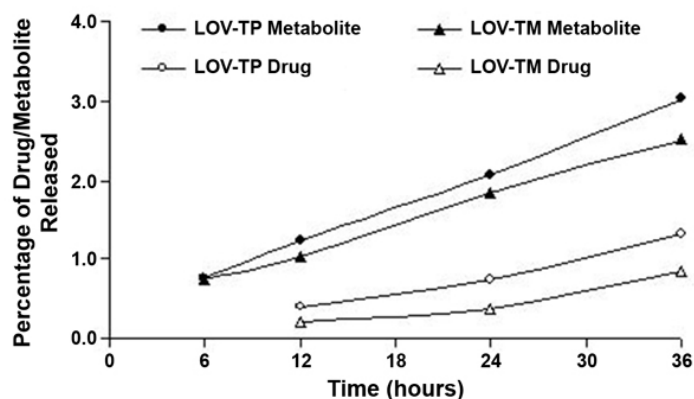


Figure 4. In vitro release of lovastatin (drug) and lovastatin hydroxy acid (metabolite) from lovastatin SLN of TM and TP in phosphate buffer pH 6.8. SLN indicates solid lipid nanoparticles; LOV, lovastatin; TM, trimyrustin; TP, tripalmitin.

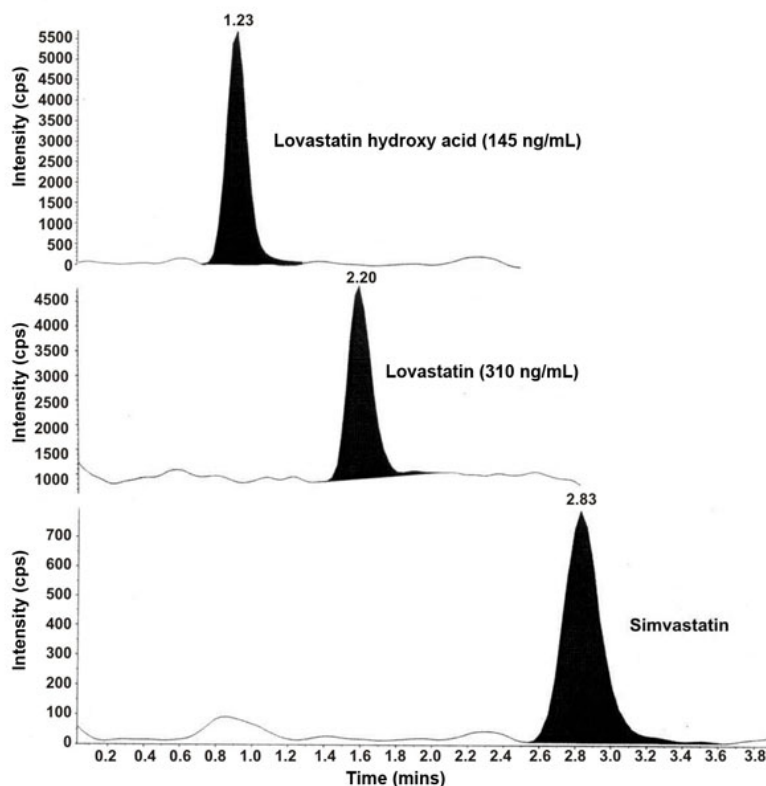


Figure 5. Liquid chromatography-mass spectroscopy/mass spectroscopy chromatograms obtained from plasma sample collected at 60 minutes.

dependent. There was no burst release of lovastatin, which indicated the absence of lovastatin on the surface of the nanoparticles. Thus, the very slow release of lovastatin and the fact that the percentages released were low suggest that lovastatin was homogeneously dispersed in the lipid matrix and that lovastatin SLN was stable in phosphate buffer pH 6.8.

Intraduodenal Administration

For bioavailability studies, LOV-TP was selected because it had a smaller particle size (65.6 ± 0.3 nm) than LOV-TM (89.8 ± 0.9 nm). Typical LC-MS/MS chromatograms of lovastatin hydroxy acid, lovastatin, and simvastatin from rat plasma collected at 60 minutes of intraduodenal administration of LOV-TP are presented in Figure 5. Following intraduodenal administration of the LOV-suspension, the average peak plasma concentrations of lovastatin hydroxy acid and lovastatin obtained were 56.4 ± 6.7 and 96.1 ± 4.4 ng/mL at 120 minutes, whereas in the case of LOV-TP, concentrations were 197.2 ± 25.7 and 323.9 ± 85.5 ng/mL at 60 minutes (Figure 6). Triglycerides of an SLN formulation enhance lymph formation and simultaneously promote lymph flow rate. This might be the reason for the shorter T_{max} for SLN than for the suspension. The T_{max} of the drug and the metabolite were the same (Table 3) because the lactone ring of lovastatin readily hydrolyzes to form lovastatin

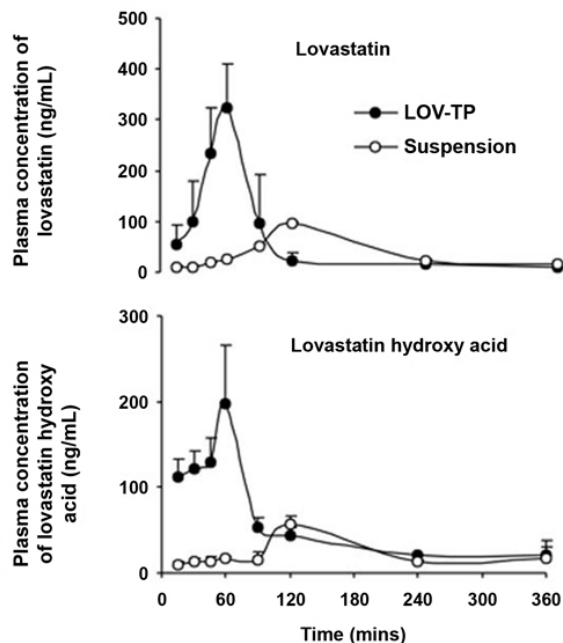


Figure 6. Mean plasma concentration of lovastatin and lovastatin hydroxy acid–time curves after intraduodenal administration of LOV-TP to rats with a dose of 10 mg/kg ($n = 3$). LOV indicates lovastatin; TP, tripalmitin.

Table 3. Pharmacokinetic Parameters (mean \pm SD, $n = 3$) of Lovastatin and Lovastatin Hydroxy Acid After Intraduodenal Administration of Lovastatin SLN of Tripalmitin and Lovastatin Suspension (10 mg/kg) to Rats*

Parameter	Lovastatin		Lovastatin Hydroxy Acid	
	SLN	Suspension	SLN	Suspension
C_{\max} (ng/mL)	323.9 \pm 85.5 \dagger	96.1 \pm 4.4	197.2 \pm 25.7 \dagger	56.4 \pm 6.7
T_{\max} (min)	60	120	60	120
AUC _(0-∞) (ng h/mL)	436.2 \pm 31.83 \ddagger	252.1 \pm 29.97	371.0 \pm 53.4 \ddagger	112.5 \pm 15.5
Fr (%)	173.0	100	323.7	100
$T_{1/2}$ (h)	3.0 \pm 0.7 \S	1.6 \pm 0.258	2.5 \pm 0.2 \ddagger	0.8 \pm 0.1
MRT (h)	3.4 \pm 0.37	2.8 \pm 0.9	3.4 \pm 0.8	2.4 \pm 0.1
CL/F (L/h/kg)	0.024 \pm 0.006 \S	0.040 \pm 0.005	0.027 \pm 0.01 \ddagger	0.088 \pm 0.012

*Statistical significances with SLN vs suspension are $\dagger P < .001$, $\ddagger P < .01$, and $\S P < .05$. SLN indicates solid lipid nanoparticles; C_{\max} , maximum plasma concentration; T_{\max} , time to reach C_{\max} ; AUC, area under the plasma concentration–time curve; Fr, relative bioavailability; $T_{1/2}$, elimination half-life; MRT, mean residence time; CL/F, clearance.

hydroxy acid in alkaline conditions. Elimination half-lives of the drug and the metabolite were higher for LOV-TP than for LOV-suspension (Table 3). The AUC(0– ∞) of lovastatin and lovastatin hydroxy acid for LOV-TP was 436.2 \pm 31.83 and 371.0 \pm 53.4 ng h/mL, whereas for LOV-suspension it was 252.1 \pm 29.97 and 112.5 \pm 15.5 ng h/mL, respectively. The difference in the AUC of lovastatin and lovastatin hydroxy acid for the LOV-TP compared with the LOV-suspension, with LOV-TP's being higher, is statistically significant ($P < .01$). The relative bioavailability of lovastatin hydroxy acid and lovastatin for LOV-TP was 323.7% and 173.0%, respectively, when compared with LOV-suspension.

The increased AUC(0– ∞) and relative bioavailability of lovastatin SLN might not be due to the amorphous form of lovastatin (confirmed by DSC and PXRD studies), because in vitro stability studies showed very slow release of lovastatin in spite of its amorphous form. Higher relative bioavailability would be due to avoidance of first-pass hepatic metabolism by intestinal lymphatic transport, which circumvents the liver. The dose of the lovastatin SLN needs to be corrected in accordance with increased bioavailability, to minimize its dose-related adverse effects, such as hepatotoxicity and myopathy. Lymphatic transport of lovastatin incorporated into SLN might have been contributed to via 1 of 2 possible mechanisms. First, exogenously administered triglycerides are digested by the action of pancreatic lipase/colipase digestive enzymes in the small intestine and absorbed into enterocytes. After absorption, long-chain fatty acids or lipids are biosynthesized into triglyceride-rich lipoprotein particles (chylomicrons), which are secreted into intestinal lymph. The size of intestinal lipoproteins precludes their absorption into the blood capillaries, and therefore they are secreted into the lymph. Second, the cellular lining of the gastrointestinal tract is composed of absorptive enterocytes interspersed with membranous epithelial (M) cells. M cells that cover lymphoid aggregates, known as Peyer's patches, take up microparticles by a combination of endocytosis or transcytosis.^{24,25} The important characteristics of nanoparticles for their uptake are optimum

size (10–100 nm), hydrophobicity, and surface charge.^{26,27} For example, the uptake of fluorescent polystyrene microparticles of size ranging from 0.1 to 3.0 μm into Peyer's patches of rats was dependent on both the size and the non-ionic nature of the particles. Uptake of many colloidal polymeric carriers across the intestinal mucosa²⁸ has been shown to occur via Peyer's patches or isolated lymphoid follicles after oral administration.²⁹ In addition to the size of LOV-TP (66 nm), its hydrophobic surface, imparted by phosphatidylcholine, might have influenced the SLN uptake by Peyer's patches. These results are supported by the literature—that is, nanospheres prepared from an oil-in-water microemulsion containing phosphatidylcholine as the surfactant favored passage of SLN through the intestinal wall after duodenal administration.^{6,11} Unfortunately, we could not collect the lymph from the rats after administration of the formulations. Analysis of lymph at regular intervals for lovastatin and its metabolites could have provided more meaningful information and support for our assumption of lymphatic transport.

CONCLUSIONS

Homogenization followed by ultrasonication is suitable for producing SLN ranging in size from 60 to 119 nm. Lipophilic drugs like lovastatin can be successfully loaded in the triglycerides (TM and TP). DSC and PXRD studies revealed that lovastatin is in an amorphous state and triglycerides are in the β' form in SLN. Stability studies indicated that lovastatin SLN display a satisfactory size and entrapment efficiency. Thus, SLN provide controlled release of drug, and these systems are preferred as drug carriers for lipophilic drugs to overcome these drugs' oral bioavailability problems.

REFERENCES

1. Yang S, Zhu J, Lu Y, Liang B, Yang C. Body distribution of camptothecin solid lipid nanoparticles after oral administration. *Pharm Res.* 1999;16:751–757.

2. Lennernas H, Fager G. Pharmacodynamics and pharmacokinetics of the HMG-CoA reductase inhibitors. Similarities and differences. *Clin Pharmacokinet.* 1997;32:403–425.
3. Khoo SM, Humberstone AJ, Porter CJH, Edwards GA, Charman WN. Formulation design and bioavailability assessment of lipidic self-emulsifying formulations of halofantrine. *Int J Pharm.* 1998;167:155–164.
4. Hauss DJ, Fogal SE, Ficorilli JV, et al. Lipid-based delivery systems for improving the bioavailability and lymphatic transport of a poorly water soluble LTB₄ inhibitor. *J Pharm Sci.* 1998;87:164–169.
5. Delie F. Evaluation of nano- and microparticle uptake by the gastrointestinal tract. *Adv Drug Deliv Rev.* 1998;34:221–233.
6. Bargoni A, Cavalli R, Caputo O, Fundaro A, Gasco MR, Zara GP. Solid lipid nanoparticles in lymph and plasma after duodenal administration to rats. *Pharm Res.* 1998;15:745–750.
7. Eldridge JH, Hammond CJ, Meulbrock JA, Staas JK, Gilley RM, Tice TR. Controlled vaccine release in the gut-associated lymphoid tissue, I: orally administered biodegradable microspheres target the Peyer's patches. *J Control Release.* 1990;11:205–214.
8. Pappo J, Ermak TM, Steger HJ. Monoclonal antibody directed targeting of fluorescent polystyrene microspheres to Peyer's patch M cells. *Immunology.* 1991;73:277–280.
9. Jepson MA, Simmons NL, O'Hagan DT, Hirst BH. Comparison of poly(DL-lactide-co-glycolide) and polystyrene microsphere targeting to intestinal M cells. *J Drug Target.* 1993;1:245–249.
10. Nishioka Y, Yoshino H. Lymphatic targeting with nanoparticulate system. *Adv Drug Deliv Rev.* 2001;47:55–64.
11. Cavalli R, Bargoni A, Podio V, Muntoni E, Zara GP, Gasco MR. Duodenal administration of solid lipid nanoparticles loaded with different percentages of tobramycin. *J Pharm Sci.* 2003;92:1085–1094.
12. Venkateswarlu V, Manjunath K. Preparation, characterization and in vitro release kinetics of clozapine solid lipid nanoparticles. *J Control Release.* 2004;95:627–638.
13. Wu Y, Zhao J, Henion J, Korfmacher WA, Lapiguera AP, Lin CC. Microsample determination of lovastatin and its hydroxy acid metabolite in mouse and rat plasma by liquid chromatography/ion spray tandem mass spectrometry. *J Mass Spectrom.* 1997;32:379–387.
14. Rajh SJ, Kreft S, Strukelj B, Vrecer F. Comparison of CE and HPLC methods for determining lovastatin and its oxidation products after exposure to an oxidative atmosphere. *Croat Chem Acta.* 2003;76:263–268.
15. Westesen K, Siekmann B, Koch MHJ. Investigations on the physical state of lipid nanoparticles by synchrotron radiation x-ray diffraction. *Int J Pharm.* 1993;93:189–199.
16. Staggers JE, Hermell O, Stafford RJ, Carey MC. Physical-chemical behaviour of dietary and biliary lipids during intestinal digestion and absorption, I: phase behavior and aggregation states of model lipid systems patterned after aqueous duodenal contents of healthy adult human beings. *Biochemistry.* 1990;29:2028–2040.
17. Yang SC, Zhu JB. Preparation and characterization of camptothecin solid lipid nanoparticles. *Drug Dev Ind Pharm.* 2002;28:265–274.
18. Freitas C, Muller RH. Correlation between long-term stability of solid lipid nanoparticles (SLNTM) and crystallinity of the lipid phase. *Eur J Pharm Biopharm.* 1999;47:125–132.
19. zur Muhlen A, Schwarz C, Mehenert W. Solid lipid nanoparticles (SLN) for controlled drug delivery—drug release and release mechanisms. *Eur J Pharm Biopharm.* 1998;45:149–155.
20. Jennings V, Thunemann AF, Gohla SH. Characterization of a novel solid lipid nanoparticle carrier system based on binary mixtures of liquid and solid lipids. *Int J Pharm.* 2000;199:167–177.
21. Jesser WA, Shneck RZ, Gile WW. Solid-liquid equilibria in nanoparticles of Pb-Bi alloys. *Phys Rev B.* 2004;69:1–13.
22. Cavalli R, Aquilano D, Carloti ME, Gasco MR. Study by x-ray powder diffraction and differential scanning calorimetry of two model drugs, phenothiazine and nifedipine, incorporated into lipid nanoparticles. *Eur J Pharm Biopharm.* 1995;41:329–333.
23. Cavalli R, Caputo O, Carloti ME, Trotta M, Scarnecchia C, Gasco MR. Sterilization and freeze-drying of drug-free and drug-loaded solid lipid nanoparticles. *Int J Pharm.* 1997;148:47–54.
24. Norris DA, Puri N, Sinko PJ. The effect of physical barriers and properties on the oral absorption of particulates. *Adv Drug Deliv Rev.* 1998;34:135–154.
25. Andrianov AK, Payne LG. Polymeric carriers for oral uptake of microparticulates. *Adv Drug Deliv Rev.* 1998;34:155–170.
26. Swartz MA. The physiology of the lymphatic system. *Adv Drug Deliv Rev.* 2001;50:3–20.
27. Florence AT, Hillery AM, Hussain N, Jani PU. Nanoparticles as carriers for oral peptide absorption: studies on particle uptake and fate. *J Control Release.* 1995;36:39–46.
28. Kreuter J. Peroral administration of nanoparticles. *Adv Drug Deliv Rev.* 1991;7:71–86.
29. Florence AT, Hillery M, Jani PU. Factors affecting the oral uptake and translocation of polystyrene nanoparticles: histological and analytical evidence. *J Drug Target.* 1995;3:65–70.